# YUCCA MOUNTAIN 2008 PERFORMANCE ASSESSMENT: UNCERTAINTY AND SENSITIVITY ANALYSIS FOR EXPECTED DOSE

C.W. Hansen[1], K. Brooks[2], J.W. Groves[3], J.C. Helton[1], K.P. Lee[4], C.J. Sallaberry[1], W. Statham[4], C. Thom[5]
[1]*Sandia National Laboratories, Albuquerque, NM 87185-0776,* cwhanse@sandia.gov
[2]*Sala Associates,* [3]*INTERA,* [4]*Areva Federal Services, LLC,* [5]*Beckman & Associates, Inc*

*Uncertainty and sensitivity analyses of the expected dose to the reasonably maximally exposed individual in the 2008 Yucca Mountain performance assessment are presented. Uncertainty results are obtained with Latin hypercube sampling of epistemic uncertain inputs, and partial rank correlation coefficients are used to illustrate sensitivity analysis results.*

## I. INTRODUCTION

A core requirement in 10 CFR 63 for the proposed Yucca Mountain (YM) repository for high level radioactive waste is that the estimated mean dose to the reasonably maximally exposed individual (RMEI) is to be less than 15 mrem/yr for the time period [0, $10^4$ yr] after repository closure. In addition, proposed regulations require the median dose to the RMEI to be less than 350 mrem/yr for the time period [$10^4$, $10^6$ yr] after repository closure.[1]

In the 2008 performance assessment (PA) for the proposed YM repository, the indicated mean and median doses are obtained by first calculating a distribution of time-dependent expected doses that result from aleatory uncertainty (i.e., the perceived randomness of future occurrences such as early waste package and drip shield failures, igneous events, seismic events). Then, the desired mean and median doses are obtained from the distribution of time-dependent expected doses.[2]

Specifically, a Latin hypercube sample (LHS) $\mathbf{e}_1$, $\mathbf{e}_2$, …, $\mathbf{e}_n$ of size $n$ = 300 was generated from the epistemically uncertain analysis inputs chosen for consideration. Next, a time-dependent expected dose $\bar{D}(\tau \mid \mathbf{e}_i)$ was determined for each of the 300 LHS elements, with each time-dependent expected dose deriving from integration over the possible realizations of aleatory uncertainty (i.e., numbers and properties of early waste package and early drip shield failures, numbers and properties of igneous events, numbers and properties of seismic events). Additionally, the time-dependent dose for nominal conditions (i.e., futures in which no early failures, seismic or igneous events occur) is also computed. Thus, expected doses $\bar{D}_C(\tau \mid \mathbf{e}_i)$ were calculated individually for the following six scenario classes: (i) $\bar{D}_{EW}(\tau \mid \mathbf{e}_i)$ with $C = EW$ for the early waste package (WP) failure scenario class $\mathcal{A}_{EW}$, (ii) $\bar{D}_{ED}(\tau \mid \mathbf{e}_i)$ with $C=ED$ for the early drip shield (DS) failure scenario class $\mathcal{A}_{ED}$, (iii) $\bar{D}_{II}(\tau \mid \mathbf{e}_i)$ with $C=II$ for the igneous intrusive scenario class $\mathcal{A}_{II}$, (iv) $\bar{D}_{IE}(\tau \mid \mathbf{e}_i)$ with $C=IE$ for the igneous eruptive scenario class $\mathcal{A}_{IE}$, (v) $\bar{D}_{SG}(\tau \mid \mathbf{e}_i)$ with $C=SG$ for the seismic ground motion scenario class $\mathcal{A}_{SG}$, and (vi) $\bar{D}_{SF}(\tau \mid \mathbf{e}_i)$ with $C=SF$ for the seismic fault displacement scenario class $\mathcal{A}_{SF}$, as well as (vii) $D_N(\tau \mid \mathbf{e}_i)$ with $C=N$ for the nominal scenario class $\mathcal{A}_N$ (see Ref. 2, Table I, for formal definitions of the individual scenario classes). Summing the preceding seven time-dependent doses for corresponding LHS elements produces $\bar{D}(\tau \mid \mathbf{e}_i)$.

Finally, the mean dose $\bar{\bar{D}}(\tau)$ was approximated by the point-wise vertical average of the 300 time-dependent expected dose curves $\bar{D}(\tau \mid \mathbf{e}_i)$, and the median dose $Q_{E,0.5}[\bar{D}(\tau \mid \mathbf{e})]$ was defined analogously as the point-wise median of the expected dose curves.[2] Thus, the mean dose curve $\bar{\bar{D}}(\tau)$ is an expectation over the epistemic uncertainty in expected dose, and the median dose curve $Q_{E,0.5}[\bar{D}(\tau \mid \mathbf{e})]$ is a median over the epistemic uncertainty in expected dose.

The indicated mean and median doses are used in assessing compliance of results obtained in the YM 2008 PA with the requirements for the [0, $10^4$ yr] and [$10^4$, $10^6$ yr] time periods, respectively.[1]

Uncertainty and sensitivity analysis results for expected dose and associated analysis insights are presented and discussed. Specifically, results are first presented for the individual scenario classes. Then, the outcome of summing the results for the individual scenario classes is presented. Results presented herein are derived from calculations performed separately for the [0, $10^4$ yr] and [0, $10^6$ yr] time periods with the TSPA-LA Model.[3] This presentation provides results for each scenario class (except for the nominal scenario class) for the time period [0, $2\times10^4$ yr], as well as for the

summation over scenario classes for both time periods. The dose to the RMEI for the nominal scenario class for the time period [0, $2\times10^4$ yr] is identically zero; results for the time period [0, $10^6$ yr] are presented elsewhere.[4] Discussion of uncertainty results for scenario classes important in the time period [0, $10^6$ yr] is provided in other presentations.[1, 5] Sensitivity analysis techniques employed herein are similar to those employed in analysis of physical processes simulated in the TSPA-LA model.[4]

## II. CONCEPTUAL BASIS

As described in a preceding presentation[2] and in more detail in an extensive analysis report[3], the conceptual structure and computational organization of the YM 2008 PA involves three basic entities: (EN1) a characterization of the uncertainty in the occurrence of future events that could affect the performance of the repository; (EN2) models for predicting the physical behavior and evolution of the repository; and (EN3) a characterization of the uncertainty associated with analysis inputs that have fixed but imprecisely known values. The designators aleatory and epistemic are commonly used for the uncertainties characterized by entities (EN1) and (EN3), respectively. Formally, (EN1) is defined by a probability space ($\mathcal{A}$, A, $p_A$) (Ref. 2, Sect. III); (EN2) corresponds to a very complex function that predicts the time-dependent behavior of many different physical properties associated with the evolution of the YM repository system[3, 5, 6, 7]; and (EN3) is defined by a probability space ($\mathcal{E}$, E, $p_E$) (Ref.2, Sect. III).

In the context of this presentation, (EN2) corresponds to the functions $D(\tau \mid \mathbf{a}, \mathbf{e})$ and $D_C(\tau \mid \mathbf{a}, \mathbf{e})$ for $C = EW$, $ED$, $II$, $IE$, $SG$ and $SF$ that define dose to the RMEI at time $\tau$ conditional on elements $\mathbf{a}$ and $\mathbf{e}$ of $\mathcal{A}$ and $\mathcal{E}$, respectively. Specifically, $D(\tau \mid \mathbf{a}, \mathbf{e})$ is the dose to the RMEI at time $\tau$ from all disruptions associated with $\mathbf{a}$, and $D_C(\tau \mid \mathbf{a}, \mathbf{e})$ is the dose to the RMEI at time $\tau$ that derives only from the disruptions associated with $\mathbf{a}$ that are also associated with the scenario class designated by $C$.

In turn, $\bar{D}(\tau \mid \mathbf{e})$ and $\bar{D}_C(\tau \mid \mathbf{e})$ are defined by integrals of $D(\tau \mid \mathbf{a}, \mathbf{e})$ and $D_C(\tau \mid \mathbf{a}, \mathbf{e})$ over $\mathcal{A}$ conditional on the element $\mathbf{e}$ of $\mathcal{E}$ (Ref. 2, Sect. IV). Similarly, the mean $\bar{\bar{D}}(\tau)$, the $q$ quantile $Q_{E,q}[\bar{D}(\tau \mid \mathbf{e})]$ (e.g., $q = 0.05, 0.5, 0.95$) and the median $Q_{E,0.5}[\bar{D}(\tau \mid \mathbf{e})]$ (i.e., $q = 0.5$) are defined by integrals over $\mathcal{E}$ (Ref. 2, Sect. IV). Corresponding results $\bar{\bar{D}}_C(\tau)$, $Q_{E,q}[\bar{D}_C(\tau \mid \mathbf{e})]$ and $Q_{E,0.5}[\bar{D}_C(\tau \mid \mathbf{e})]$ for individual scenario classes are defined in the same manner.

## III. EARLY FAILURE SCENARIO CLASSES

As indicated in Sects. I and II, two early failure scenario classes are considered in the 2008 YM PA: the early DS scenario class $\mathcal{A}_{ED}$ and the early WP scenario class $\mathcal{A}_{EW}$. The occurrence of early DS failures and early WP failures are modeled with binomial probability distributions with defining parameters *PROBDSEF* and *PROBWPEF* (see Table I). The individual DS failure probability *PROBDSEF* applies to all DSs in the repository. Similarly, the individual WP failure probability *PROBWPEF* applies to all WPs in the repository. As modeled, early failure of DSs and WPs allow radionuclide transport from the affected WPs to begin soon after repository closure.[6]

TABLE I. Variables Appearing in Sensitivity Analyses for *EXPDOSE* in Figs. 1-4.

| |
|---|
| *SCCTHRP:* Residual stress threshold for SCC nucleation of Alloy 22 (as a percentage of yield strength in MPa) (dimensionless). |
| *DASHAVG:* Mass median ash particle diameter (cm). |
| *DDIVIDE:* Diffusivity of radionuclides in divides of the Fortymile Wash fan (RMEI location) ($cm^2/yr$). |
| *DSNFMASS:* Scale factor used to characterize uncertainty in radionuclide content of DSNF (dimensionless). |
| *EP1LOWPU:* Logarithm of the scale factor used to characterize uncertainty in plutonium solubility at an ionic strength below 1 molal (dimensionless). |
| *IGRATE:* Frequency of intersection of the repository footprint by a volcanic event ($yr^{-1}$). |
| *IGERATE:* Frequency of occurrence of volcanic eruptive events ($yr^{-1}$). |
| *INFIL:* Pointer variable for determining infiltration conditions: $10^{th}$, $30^{th}$, $50^{th}$ or $90^{th}$ percentile infiltration scenario (dimensionless). |
| *INHLTPV:* Pointer variable for short-term inhalation dose conversion factor for volcanic ash exposure (dimensionless). |
| *MICC14:* Groundwater Biosphere Dose Conversion Factor (BDCF) for $^{14}C$ in modern interglacial climate ((Sv/year)/($Bq/m^3$)). |
| *MICTC99:* Groundwater Biosphere Dose Conversion Factor (BDCF) for $^{99}Tc$ in modern interglacial climate ((Sv/year)/($Bq/m^3$)). |
| *PROBDSEF:* Probability for undetected defects in drip shields (dimensionless). |
| *PROBWPEF:* Probability for the undetected defects in waste packages (dimensionless). |
| *SEEPPRM:* Logarithm of the mean fracture permeability in lithophysal rock units (dimensionless). |
| *SEEPUNC:* Uncertainty factor to account for small-scale heterogeneity in fracture permeability (dimensionless). |
| *SZCOLRAL:* Logarithm of colloid retardation factor in alluvium (dimensionless). |
| *SZFIPOVO:* Logarithm of flowing interval porosity in volcanic units (dimensionless). |
| *SZGWSPDM:* Logarithm of the scale factor used to characterize uncertainty in groundwater specific discharge (dimensionless). |
| *THERMCON:* Selector variable for one of three host-rock thermal conductivity scenarios (low, mean, and high) (dimensionless). |
| *WDGCA22:* Temperature dependent slope term of Alloy 22 general corrosion rate (K). |

The time-dependent expected doses to the RMEI from early DS failure ($\bar{D}_{ED}(\tau \mid \mathbf{e}_i)$) and from early WP

failure ($\bar{D}_{EW}(\tau \mid \mathbf{e}_i)$) for the individual LHS elements $\mathbf{e}_i$, $i$ = 1, 2, …, 300, are shown in Figs. 1a and 1c. Fig. 1c shows increases in $\bar{D}_{EW}(\tau \mid \mathbf{e}_i)$ starting at approximately $10^4$ yr, corresponding to the arrival of radionuclides from early-failed commercial spent nuclear fuel WPs. Because these WPs are hotter than other WPs, formation of continuous liquid pathways occurs later[6], delaying release of radionuclides from these early-failed WPs.

As shown by the spread of the individual curves, considerable uncertainty exits with respect to the values for $\bar{D}_{ED}(\tau \mid \mathbf{e}_i)$ and $\bar{D}_{EW}(\tau \mid \mathbf{e}_i)$. Sensitivity analyses for $\bar{D}_{ED}(\tau \mid \mathbf{e}_i)$ and $\bar{D}_{EW}(\tau \mid \mathbf{e}_i)$ based on partial rank correlation coefficients (PRRCs; see Ref. 4, Sect. II) are presented in Figs. 1b and 1d (see Table I for definitions of individual variables). The dominant variables with respect to the uncertainty in $\bar{D}_{EW}(\tau \mid \mathbf{e})$ and $\bar{D}_{ED}(\tau \mid \mathbf{e})$ are *PROBWPEF* and *PROBDSEF*, respectively, with $\bar{D}_{EW}(\tau \mid \mathbf{e})$ and $\bar{D}_{ED}(\tau \mid \mathbf{e})$ increasing as *PROBWPEF* and *PROBDSEF* increase, because the expected number of early failures increase. After *PROBWPEF* and *PROBDSEF*, the PRCCs indicate smaller effects for a number of additional variables that influence the movement of water through the natural barriers of the repository system.

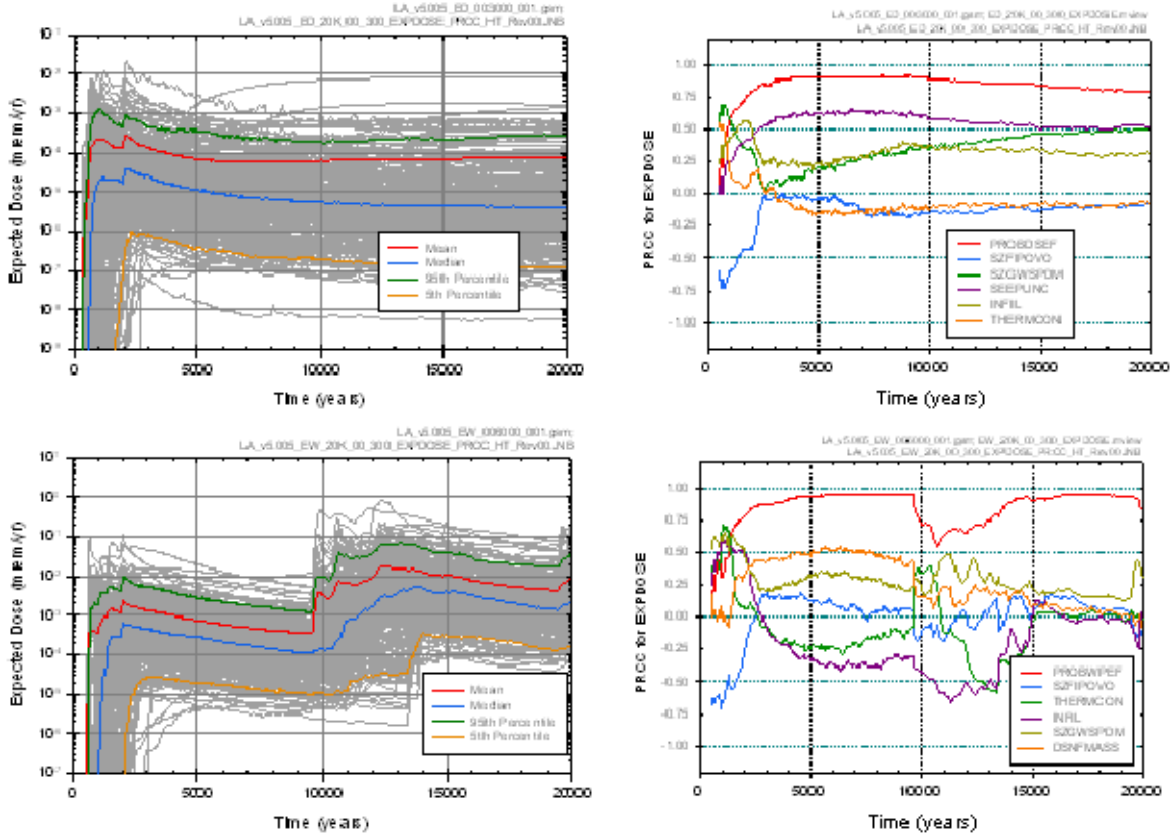


Fig. 1. Expected dose to RMEI (mrem/yr) over $[0, 2\times10^4$ yr] for all radioactive species resulting from early failures: (a, b) $\bar{D}_{ED}(\tau \mid \mathbf{e})$ and associated PRCCs for early DS failure (Ref. 3, Fig. K5.7.1-1[a]), and (c, d) $\bar{D}_{EW}(\tau \mid \mathbf{e})$ and associated PRCCs for early WP failure (Ref. 3, Fig. K5.7.2-1[a]).

## IV. IGNEOUS SCENARIO CLASSES

Two igneous scenario classes are considered in the YM 2008 PA: the igneous intrusion scenario class $\mathcal{A}_{II}$ and the igneous eruptive scenario class $\mathcal{A}_{IE}$. The occurrence of igneous intrusion events and igneous eruptive events are modeled by Poisson processes with rates defined by *IGRATE* and *IGERATE* (See Table I). Further, an igneous intrusion event is assumed to destroy all WPs in the repository, and an igneous eruptive event ejects the contents of a small number of WPs into the atmosphere.[5]

The time-dependent expected doses to the RMEI from igneous intrusions ($\bar{D}_{II}(\tau \mid \mathbf{e}_i)$) and from igneous eruptions ($\bar{D}_{IE}(\tau \mid \mathbf{e}_i)$) for the individual LHS elements

$\mathbf{e}_i$, $i$ = 1, 2, …, 300, are shown in Figs. 2a and 2c. The smoothness evident in these curves results from the use of quadrature procedures in the evaluation of expected dose.[2] As shown by the spread of the individual curves, considerable uncertainty exits with respect to the values for $\bar{D}_{II}(\tau \mid \mathbf{e}_i)$ and $\bar{D}_{IE}(\tau \mid \mathbf{e}_i)$. Sensitivity analyses for $\bar{D}_{II}(\tau \mid \mathbf{e}_i)$ and $\bar{D}_{IE}(\tau \mid \mathbf{e}_i)$ based on PRRCs are presented in Figs. 2b and 2d (see Table I for definitions of individual variables). The dominant variables with respect to the uncertainty in $\bar{D}_{II}(\tau \mid \mathbf{e}_i)$ and $\bar{D}_{IE}(\tau \mid \mathbf{e}_i)$ are the occurrence rates *IGRATE* and *IGERATE*, respectively, with $\bar{D}_{II}(\tau \mid \mathbf{e})$ and $\bar{D}_{IE}(\tau \mid \mathbf{e})$ increasing as *IGRATE* and *IGERATE* increase.

The physical processes associated with igneous intrusive events and igneous eruptive events that result in dose to the RMEI are very different.[5] As a result, the variables selected after *IGRATE* and *IGERATE* in Figs. 2b and 2d are very different. Specifically, analysis for $\bar{D}_{II}(\tau \mid \mathbf{e})$ in Fig. 2b indicates effects for variables that influence the movement of water through the natural system (*SZGWSPDM*, *INFIL*, *SZFIPOVO* and *SZCOLRAL*) and the contribution of $^{99}$Tc to dose to the RMEI (*MICTC99*). The analysis for $\bar{D}_{IE}(\tau \mid \mathbf{e})$ in Fig. 2d indicates effects for variables related to the uncertainty in dose to the RMEI by inhalation of contaminated particles (*INHLTPV*), the diffusion of radionuclides downward out of surface soils (*DDIVIDE*), the mass of radionuclides in waste packages (*CSNFMASS*), and the attachment of waste particles to ash particles (*DASHAVG*).

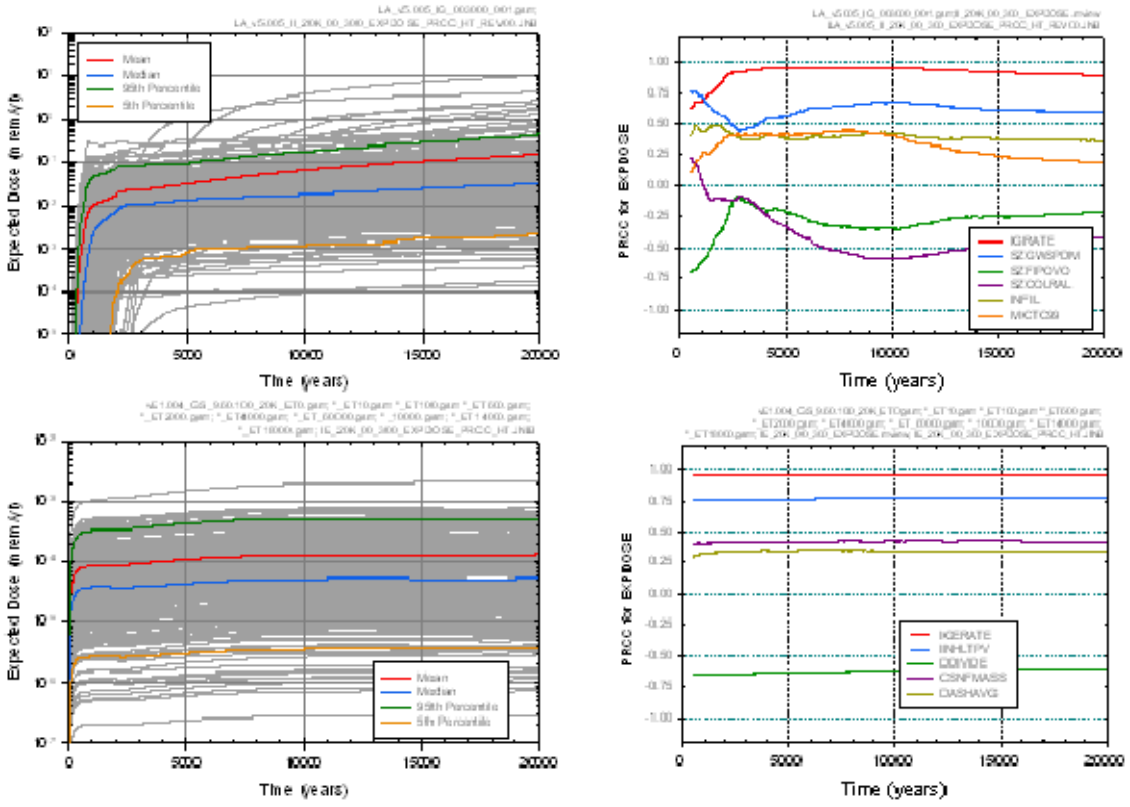


Fig. 2. Expected dose to RMEI (mrem/yr) over $[0, 2\times10^4$ yr] for all radioactive species resulting from igneous events: (a, b) $\bar{D}_{II}(\tau \mid \mathbf{e})$ and associated PRCCs for igneous intrusive events (Ref. 3, Fig. K6.7.1-1[a]), and (c, d) $\bar{D}_{IE}(\tau \mid \mathbf{e})$ and associated PRCCs for early igneous eruptive events (Ref. 3, Fig. K6.8.1-1).

## V. SEISMIC SCENARIO CLASSES

Two seismic scenario classes are considered in the 2008 YM PA: the seismic ground motion scenario class $\mathcal{A}_{SG}$ and the seismic fault displacement scenario class $\mathcal{A}_{SF}$. The occurrence of seismic ground motion events and seismic fault displacement events are modeled as Poisson processes defined by underlying hazard curves that define the annual frequencies of seismic ground

motion events and seismic fault displacement events of different sizes.[5] A seismic ground motion event that damages WPs is assumed to cause the same damage to all WPs in the repository; in contrast, a seismic fault displacement event damages a relatively small number of WPs. .

The time-dependent expected doses to the RMEI from seismic ground motion events ( $\bar{D}_{SG}(\tau \mid \mathbf{e}_i)$ ) and from seismic fault displacement events ( $\bar{D}_{SF}(\tau \mid \mathbf{e}_i)$ ) for the individual LHS elements $\mathbf{e}_i$, $i$ = 1, 2, …, 300, are shown in Figs. 3a and 3c. The spread of the individual curves shows considerable uncertainty exists with respect to the values for $\bar{D}_{SG}(\tau \mid \mathbf{e}_i)$ and $\bar{D}_{SF}(\tau \mid \mathbf{e}_i)$ . Sensitivity analyses for $\bar{D}_{SG}(\tau \mid \mathbf{e})$ and $\bar{D}_{SF}(\tau \mid \mathbf{e}_i)$ based on PRRCs are presented in Figs. 3b and 3d (see Table I for definitions of individual variables). The dominant variable with respect to the uncertainty in $\bar{D}_{SG}(\tau \mid \mathbf{e})$ is *SCCTHRP*, with $\bar{D}_{SG}(\tau \mid \mathbf{e})$ decreasing as *SCCTHRP* increases. The strong effect associated with *SCCTHRP* results because *SCCTHRP* defines the residual stress level at which WPs are considered to be damaged by seismically-induced impacts. The TSPA-LA does not represent epistemic uncertainty in the hazard curves which define the annual frequencies of seismic ground motion events, thus no variable related to the occurrence of seismic events is present in the sensitivity analysis. After *SCCTHRP*, the analyses for $\bar{D}_{SG}(\tau \mid \mathbf{e})$ indicates effects for variables that influence movement of water through the natural system (*SZFIPOVO*, *SZGWSPDM,* and *INFIL*), the mass of radionuclides in the disposed waste (*DSNFMASS*) and the contribution of $^{99}$Tc to dose to the RMEI (*MICTC99*).

For $\bar{D}_{SF}(\tau \mid \mathbf{e}_i)$ **,** effects are indicated for variables related to the movement of water through the natural system (*SZGWSPDM*, *INFIL*, *SEEPUNC*, *SZFIPOVO* and *SEEPPRM*) and the contribution of $^{99}$Tc to dose to the RMEI (*MICTC99*). However, unlike the analysis for $\bar{D}_{SG}(\tau \mid \mathbf{e})$ , no single variable dominates the uncertainty in $\bar{D}_{SF}(\tau \mid \mathbf{e}_i)$ . Because the TSPA-LA does not represent epistemic uncertainty in the hazard curve describing frequencies of fault displacement events and the number of waste packages affected by events of different magnitudes, the sensitivity analysis does not involve variables related to the occurrence of seismic fault events or the number of WPs damaged by a fault displacement event.

## VI. ALL SCENARIO CLASSES

Expected dose results for individual scenario classes are presented in Sects. III-V. As discussed in Section I, the total expected dose $\bar{D}(\tau \mid \mathbf{e})$ for all scenario classes results from adding the expected doses for the individual scenario classes. Specifically, the total expected doses $\bar{D}(\tau \mid \mathbf{e}_i)$ in Fig. 4a for the time period $[0, 2\times10^4$ yr] result from adding the expected doses in Figs. 1-3 for corresponding LHS elements $\mathbf{e}_i$, $i$ = 1, 2, …, 300. Similarly, the total expected doses $\bar{D}(\tau \mid \mathbf{e}_i)$ in Fig. 4c for the time period $[0,10^6$ yr] result from adding the expected doses for the individual scenario classes for this time period. Additional detail is provided in an extensive analysis report.[3]

In turn, the total expected doses $\bar{D}(\tau \mid \mathbf{e}_i)$ in Figs. 4a and 4c can be used to estimate mean doses $\bar{\bar{D}}(\tau)$ over aleatory and epistemic uncertainty and quantiles $Q_{Eq}[\bar{D}(\tau \mid \mathbf{e})]$ (e.g., $q$ = 0.05, 0.5, 0.95) for $\bar{D}(\tau \mid \mathbf{e})$ that derive from epistemic uncertainty. Values for $\bar{\bar{D}}(\tau)$ and $Q_{Eq}[\bar{D}(\tau \mid \mathbf{e})]$, $q$ = 0.05, 0.5, 0.95, are shown in Figs. 4a and 4b. The 2008 YM PA uses the mean dose $\bar{\bar{D}}(\tau)$ in comparisons with the 15 mrem/yr dose standard specified by the NRC for the time period $[0,10^4$ yr] and uses the median expected dose $Q_{E,0.5}[\bar{D}(\tau \mid \mathbf{e})]$ in comparisons with the 350 mrem/yr dose standard specified by the NRC for the time period $[0,10^6$ yr] .[1]

The total expected dose $\bar{D}(\tau \mid \mathbf{e})$ for the time period $[0, 2\times10^4$ yr] is primarily determined by the expected dose from seismic ground motion with a secondary contribution from the expected dose from igneous intrusion.[1] All other scenario classes have a marginal contribution to total expected dose. For the time period $[0,10^6$ yr] , expected dose from these same scenario classes primarily determine the median expected dose $Q_{E,0.5}[\bar{D}(\tau \mid \mathbf{e})]$.

The smoothness evident in the expected dose results for the time period $[0, 2\times10^4$ yr] results from the quadrature procedure used to evaluate the expected dose from seismic ground motion for this time period.[2] In contrast, the Monte Carlo procedure used to evaluate expected dose from the combination of seismic ground motion and nominal corrosion processes for the time period $[0,10^6$ yr] results in the spikes in total expected dose evident in Fig. 4c. Although these spikes could be smoothed by use of a larger sample size in the calculation, the sample sizes employed are sufficient to yield a stable estimate of the mean dose and median expected dose, as will be shown.

As shown by the spread of the results in Figs. 4a and 4c, a substantial amount of uncertainty is present in the

estimation of $\bar{D}(\tau \mid \mathbf{e})$. The sensitivity analyses in Figs. 4b and 4d indicate the variables that are giving rise to the uncertainty in $\bar{D}(\tau \mid \mathbf{e})$. The PRCCs in Fig. 4b indicate that the uncertainty in $\bar{D}(\tau \mid \mathbf{e})$ for the time interval $[0, 2\times10^4$ yr$]$ is dominated by *SCCTHRP* (see Table I for definitions of individual variables), reflecting the dominant contribution to total expected dose from the expected dose from seismic ground motion, and the importance of this variable to the expected dose from seismic ground motion. Smaller effects are evident from the frequency of igneous events (*IGRATE*), from variables that influence movement of water (*SZGWSPDM*, *SZFIPOVO*, and *INFIL*) and the contribution of $^{14}$C to dose to the RMEI (*MICC14*) (the contribution of $^{99}$Tc to dose is slightly less than the variables identified in Fig. 4b).[3] For the time period $[0, 10^6$ yr$]$, the PRCCs in Fig. 4d indicate that the three most important variables with respect to the uncertainty in $\bar{D}(\tau \mid \mathbf{e})$ for the time interval are *SCCTHRP*, *IGRATE* and *WDGCA22*. In turn, *SCCTHRP* is the dominant variable affecting the uncertainty in expected dose from seismic ground motion events; *IGRATE* is the dominant variable affecting the uncertainty in expected dose $\bar{D}_{II}(\tau \mid \mathbf{e})$ from igneous intrusive events; and *WDGCA22* is the dominant variable affecting the uncertainty in the dose $D_N(\tau \mid \mathbf{e})$ from nominal processes.[4] In addition, smaller effects are indicated for *SZGWSPDM*, *SZFIPOVO* and for uncertainty in plutonium solubility (*EP1LOWPU*).

The 2008 YM PA used a LHS of size 300 to estimate $\bar{D}(\tau \mid \mathbf{e})$ (Ref. 2, Sect V). Given that 392 epistemically uncertain variables are under consideration in the TSPA-LA model (i.e., $\mathbf{e}$ is a vector of length 392), it is reasonable to ask if this is a sufficiently large sample to obtain stable results. To answer this question, the analysis repeated three times with independently generated LHSs of size 300. As shown in Fig. 5, the values obtained for $\bar{\bar{D}}(\tau)$ and $Q_{Eq}[\bar{D}(\tau \mid \mathbf{e})]$, $q$ = 0.05, 0.5, 0.95, for these three samples are similar. Thus, an LHS of size 300 is adequate to obtain stable results for the propagation of epistemic uncertainty in the 2008 YM PA. The reader should note that the stability results summarized in Fig. 5 are from a near-final version of the TSPA-LA model, and hence are slightly different in shape and magnitude from those presented in Fig. 4.

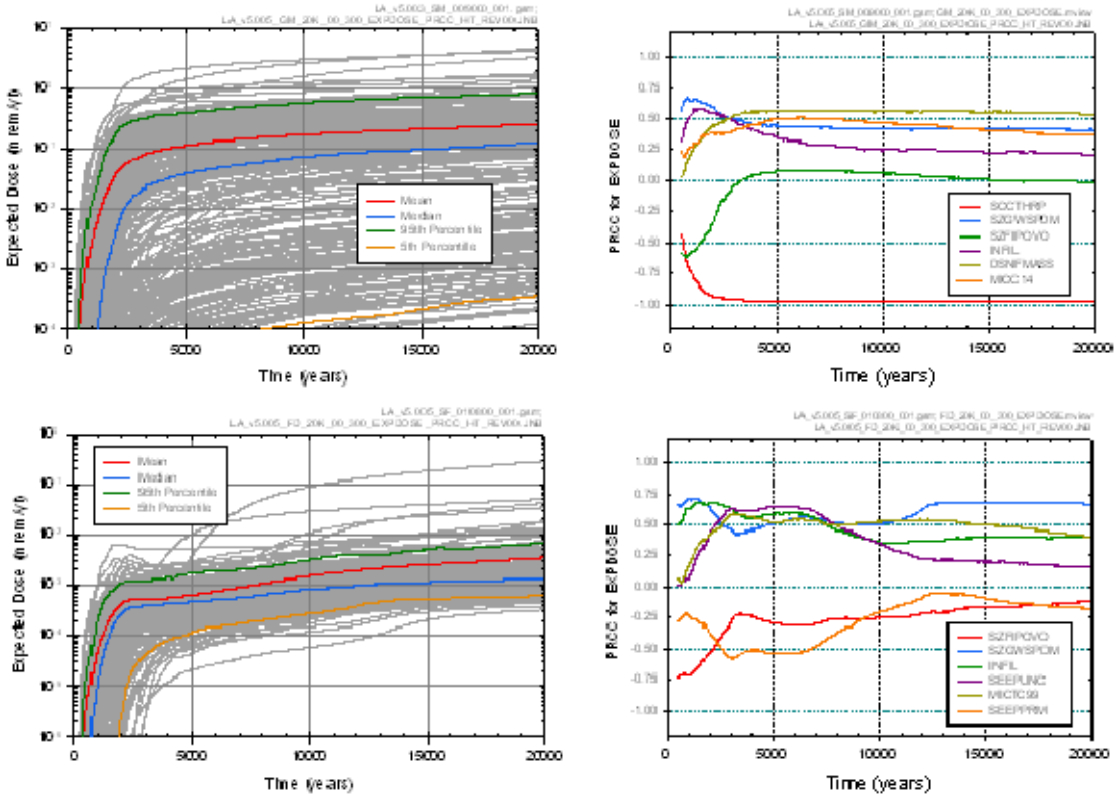

Fig. 3. Expected dose to RMEI (mrem/yr) over $[0, 2\times10^4$ yr] for all radioactive species resulting from seismic events: (a, b) $\bar{D}_{SG}(\tau \mid \mathbf{e}_i)$ and associated PRCCs for seismic ground motion events (Ref. 3, Fig. K7.7.1-1[a]), and (c, d) $\bar{D}_{SF}(\tau \mid \mathbf{e}_i)$ and associated PRCCs for seismic fault displacement events (Ref. 3, Fig. K7.8.1-1[a]).

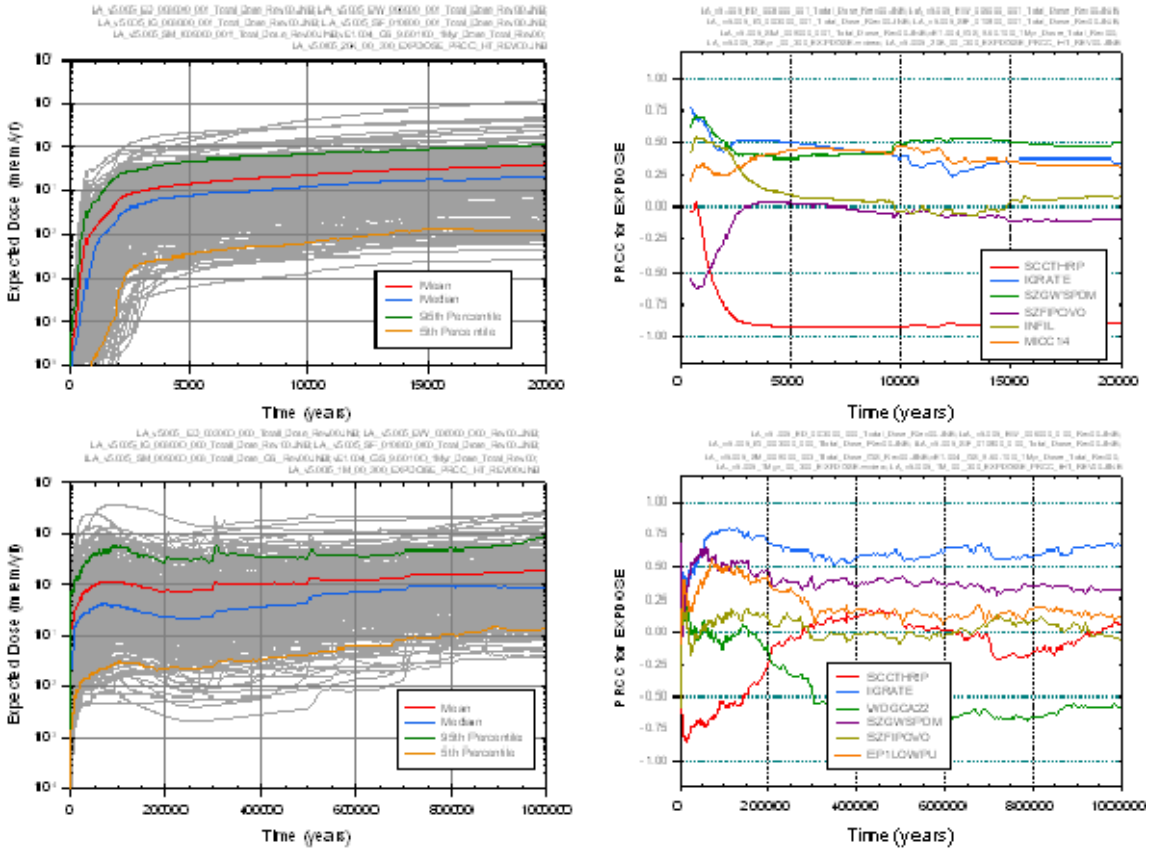


Fig. 4. Expected dose to RMEI (mrem/yr) for all radioactive species and all scenario classes: (a, b) $\bar{D}(\tau \mid \mathbf{e})$ and associated PRCCs for $[0, 2\times10^4$ yr] (Ref. 3, Fig. K8.1-1[a]), and (c, d) $\bar{D}(\tau \mid \mathbf{e})$ and associated PRCCs for $[0, 10^6$ yr] (Ref. 3, Fig. K8.2-1[a]).

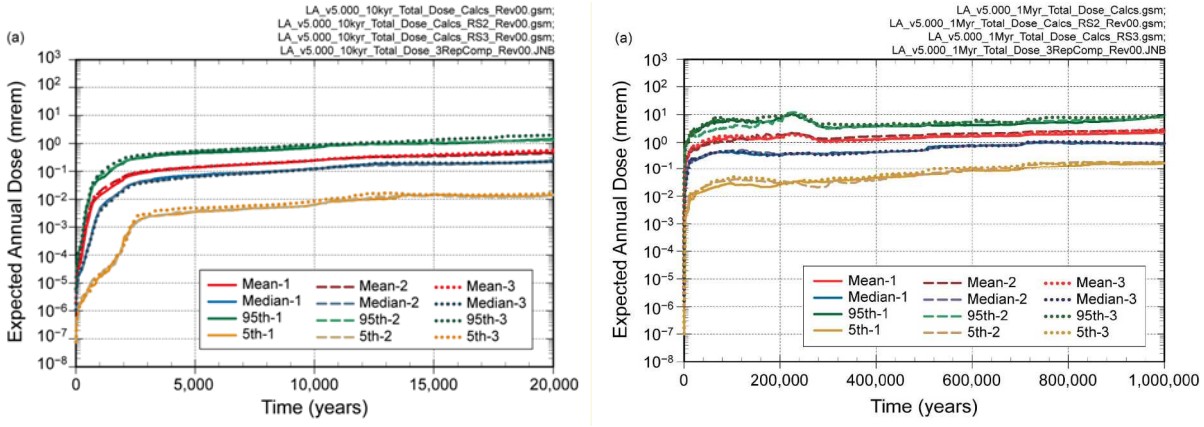


Fig. 5. Stability of estimates of expected dose $\bar{D}(\tau \mid \mathbf{e})$ to RMEI (mrem/yr) for all radioactive species and all scenario classes: (a) $[0, 2\times10^4$ yr] (Ref. 3, Fig. 7.3.1-15a), and (b) $[0, 10^6$ yr] (Ref. 3, Fig. 7.3.1-16a).

## VII. SUMMARY

Uncertainty and sensitivity analysis are important parts of the analysis of expected dose in the YM 2008 PA. These analyses showed that (i) although there is substantial uncertainty in the estimation of expected dose, the mean and median for expected dose are below regulatory standards specified by the NRC, (ii) mean and expected doses for all scenario classes are dominated by the doses arising from the seismic ground motion scenario class and the igneous intrusion scenario class for the $[0, 2\times10^4$ yr] time period and by the doses arising from nominal processes, the seismic ground motion scenario class and the igneous intrusion scenario class for the $[0,10^6$ yr] time period, (iii) the uncertainty in the expected dose from disruptive events tends to be dominated by the uncertainty in the rate of occurrence of these events, and (iv) an LHS of size 300 is adequate for the propagation of epistemic uncertainty in the YM 2008 PA. In addition, the sampling-based methods used for uncertainty and sensitivity analysis played an important role in analysis verification by allowing a detailed examination of the effects of analysis inputs on analysis results.

Additional extensive uncertainty and sensitivity analyses for dose, expected dose and many other analysis results are available in Apps. J and K of Ref. [3]

## ACKNOWLEDGMENTS

The authors thank the many hundreds of people whose work over more than two decades has contributed to this analysis. This paper benefited from review at Sandia and within the Lead Laboratory by xxx and yyy. Sandia is a multi-program laboratory operated by Sandia Corporation, a Lockheed Martin Company, for the United States Department of Energy's National Nuclear Security Administration under contract DE-AC04-94AL85000.

## REFERENCES

1. PETER N. SWIFT, KATHRYN KNOWLES, JERRY MCNEISH, CLIFFORD W. HANSEN, ROBERT L. HOWARD, ROBERT MACKINNON, AND S. DAVID SEVOUGIAN, "Yucca Mountain 2008 Performance Assessment: Summary," Proceedings of the 2008 International High-Level Radioactive Waste Management Conference, September 7-11, 2008 (this volume) (2008).

2. J. C. HELTON, C. W. HANSEN, and C. J. SALLABERRY, "Yucca Mountain 2008 Performance Assessment: Conceptual Structure and Computational Organization," Proceedings of the 2008 International High-Level Radioactive Waste Management Conference, September 7-11, 2008 (this volume) (2008).

3. SNL (Sandia National Laboratories), *Total System Performance Assessment Model/Analysis for the License Application,* MDL-WIS-PA-000005 Rev 00, AD 01 (2008).

4. C. J. SALLABERRY, A. ARAGON, A. BIER, Y. CHEN, J. GROVES, C. W. HANSEN, J. C. HELTON, S. MEHTA, S. MILLER, J. MIN, and P. VO, "Yucca Mountain 2008 Performance Assessment: Uncertainty and Sensitivity Analyses for Physical Processes," Proceedings of the 2008 International High-Level Radioactive Waste Management Conference, September 7-11, 2008 (this volume) (2008).

5. S. D. SEVOUGIAN, A. BEHIE, B. BULLARD, V. CHIPMAN, M. GROSS, and W. STATHAM, "Yucca Mountain 2008 Performance Assessment: Modeling Disruptive Events and Early Failures," *Proceedings of the 2008 International High-Level Radioactive Waste Management Conference,* September 7-11, 2008 (this volume), American Nuclear Society (2008).

6. R. J. MACKINNON, A. BEHIE, V. CHIPMAN, Y. CHEN, J. LEE, K. P. LEE, P. MATTIE, S. MEHTA, K. MON, J. SCHREIBER, S. D. SEVOUGIAN, C. STOCKMAN, and E. ZWAHLEN, "Yucca Mountain 2008 Performance Assessment: Modeling the Engineered Barrier System," Proceedings of the 2008 International High-Level Radioactive Waste Management Conference, September 7-11, 2008 (this volume) (2008).

7. P. D. MATTIE, T. HADGU, B. LESTER, A. SMITH, M. WASIOLEK, and E. ZWAHLEN, "Yucca Mountain 2008 Performance Assessment: Modeling the Natural System," *Proceedings of the 2008 International High-Level Radioactive Waste Management Conference,* September 7-11, 2008 (this volume), American Nuclear Society (2008).